Engineering Analysis with Boundary Elements 36 (2012) 30–38

Contents lists available at ScienceDirect

Engineering Analysis with Boundary Elements

journal homepage: www.elsevier.com/locate/enganabound

A Trefftz based method for solving Helmholtz problems in semi-infinite domains

Bart Bergen *, Bert Pluymers, Bert Van Genechten, Dirk Vandepitte, Wim Desmet

K.U.Leuven, Department of Mechanical Engineering, division PMA, Celestijnenlaan 300B - box 2420, B-3001 Leuven, Belgium

ARTICLE INFO

Article history:
Received 8 December 2010
Accepted 14 April 2011
Available online 9 September 2011

Keywords:
Trefftz method
Wave based method
Helmholtz problems
Semi-unbounded problems

ABSTRACT

The wave based method (WBM), which is based on an indirect Trefftz approach, is a deterministic prediction method posed as an alternative to the element-based methods. It uses wave functions, which are exact solutions of the underlying differential equation, to describe the dynamic field variables. In this way, it can avoid the pollution errors associated with the polynomial element-based approximations. As a consequence, a dense element discretization is no longer required, yielding a smaller numerical system. The resulting enhanced computational efficiency of the WBM as compared to the element-based methods has been proven for the analysis of both bounded and unbounded acoustic problems. This paper extends the applicability of the WBM to semi-infinite domains. An appropriate function set is proposed, together with a calculation procedure for both semi-infinite radiation and scattering problems, and transmission or diffraction problems containing a rigid baffle. The resulting technique is validated on two numerical examples.

1. Introduction

Ever increasing restrictive legal regulations regarding noise and vibration exposure as well as the customer's growing demand for comfort, force industrial designers to take into account the acoustic behaviour of their products in the design optimization. As *time is money* and *less is more*, Computer Aided Engineering (CAE) tools have become an essential part in the product development process. The possibility of analyzing and optimizing virtual prototypes has relaxed the need for very expensive and time-consuming physical prototype testing.

Both the finite element method (FEM) and the boundary element method (BEM) are well established deterministic CAE tools which are commonly used for the analysis of real-life acoustic problems. The FEM [1] discretizes the entire problem domain into a large but finite number of small elements. Within these elements, the dynamic response variables are described in terms of simple, polynomial shape functions. Because the FEM is based on a discretization of the problem domain into small elements, it cannot handle unbounded problems inherently. An artificial boundary is needed to truncate the unbounded problem into a bounded problem. Special techniques are then required to reduce spurious reflection of waves at the truncation boundary. Three strategies are applied to this end [2,3]: absorbing boundary conditions [4], infinite elements [5] or absorbing layers [6].

The BEM [7] is based on a boundary integral formulation of the problem. As a result, only the boundary of the considered domain has to be discretized. Within the applied boundary elements, some acoustic boundary variables are expressed in terms of simple, polynomial shape functions, similar to the FEM. Since the boundary integral formulation inherently satisfies the Sommerfeld radiation condition, the BEM is particularly suited for the treatment of problems in unbounded domains.

However, since the simple shape functions used in both the FEM and BEM are no exact solutions of the governing differential equations, a very fine discretization is required to suppress the associated pollution errors [8] and to obtain a reasonable prediction accuracy. The resulting large numerical models limit the practical applicability of these methods to low-frequency problems [9], due to the prohibitively large computational cost.

To overcome those limitations, several enhanced methods are proposed [2]. Often, those methods apply a wave-like basis for the approximation to better match the nature of the dynamic field. To this end, the spectral methods use a global basis based on oscillating functions, such as harmonics (sine and cosine) or Chebyshev polynomials [10,11]. The Trefftz methods [12] take this approach a step further, selecting the basis functions to satisfy *a priori* the governing dynamic equations. Several methods have been developed following this philosophy. The Equivalent Source Method (ESM) [13] is a prominent example, which employs a weighted distribution of particular solutions to

* Corresponding author.
E-mail address: bart.bergen@mech.kuleuven.be (B. Bergen).

0955-7997/$ - see front matter © 2011 Elsevier Ltd. All rights reserved.
doi:10.1016/j.enganabound.2011.04.007

describe the dynamic field. Many variations on this method are proposed, using different distributions and types of sources, such as acoustic point sources [14] and plane waves [15]. It is also possible to use homogeneous solutions of the governing equations in the field expansion [16]. The ability to include *a priori* known information in the numerical model often yields an improved accuracy and computational efficiency, as illustrated by several applications in various problem domains [17,18].

The wave based method (WBM) [19] is another alternative deterministic technique for the analysis of acoustic problems. The method is also based on an indirect Trefftz approach [12], in that the dynamic response variables are described using so-called wave functions which exactly satisfy the governing differential equation. In this way, no approximation error is made inside the domain. However, the wave functions may violate the boundary and continuity conditions. Enforcing the associated residual errors to zero in a weighted residual scheme yields a small system of algebraic equations. Solution of these equations results in the contribution factors of the wave functions used in the expansion of the dynamic field variables.

The WBM has been applied successfully for many steady-state structural dynamic problems [20], interior acoustic problems [21], interior vibro-acoustic problems [22,23] and exterior (vibro-)acoustic problems [24–27]. It is shown that, due to the small model size and the enhanced convergence characteristics, the WBM has a superior numerical performance as compared to the element-based methods. As a result, problems at higher frequencies may be tackled.

This paper discusses the extension of the WBM for two-dimensional (2D) acoustic analyses in semi-infinite domains. This is an important type of problem, as in many practical radiation and scattering problems the acoustic domain is truncated by a rigid baffle plane. This extension is also useful for the study of acoustic transmission and diffraction problems, in which the problem domain consists of two semi-infinite domains, connected to each other through an aperture in the baffle plane, possibly containing a structure.

This paper consists of three parts. The first part presents a mathematical problem definition of a general steady-state acoustic problem. The second part describes the WBM methodology, and proposes a function set suitable for modeling a semi-infinite domain. In the third part, the proposed formulation is applied to model two examples. The first one is a validation study considering a pulsating piston in a baffle. This allows to compare the obtained results with an analytical solution of the problem. A second example illustrates the potential to tackle diffraction problems, by considering an aperture in a baffle, shielded by a plate.

2. Problem description

Consider a general 2D unbounded acoustic problem shown in Fig. 1. The steady-state acoustic pressure inside the problem domain is governed by the inhomogeneous Helmholtz equation [28]:

$$\nabla^2 p(\boldsymbol{r}) + k^2 p(\boldsymbol{r}) = -j\rho_0\omega\delta(\boldsymbol{r},\boldsymbol{r_q})q \tag{1}$$

with ω the circular frequency and $k=\omega/c$ the acoustic wave number, j is the imaginary unit ($j=\sqrt{-1}$). The acoustic fluid is characterized by its density ρ_0 and speed of sound c. The fluid is excited by a cylindrical acoustic volume velocity source with source strength q. The problem boundary Γ constitutes two parts: the finite part of the boundary, Γ_b, and the boundary at infinity, Γ_∞. Based on the three types of commonly applied acoustic boundary conditions, the finite boundary can be further divided into three non-overlapping parts: $\Gamma_b=\Gamma_v\cup\Gamma_p\cup\Gamma_Z$. If we define the velocity operator $\mathcal{L}_v(\bullet)$ as

$$\mathcal{L}_v(\bullet) = \frac{j}{\rho_0\omega}\frac{\partial\bullet}{\partial n} \tag{2}$$

with n the local normal on the boundary, we can write the boundary condition residuals:

$$\boldsymbol{r}\in\Gamma_v : R_v = \mathcal{L}_v(p(\boldsymbol{r})) - \overline{v}_n(\boldsymbol{r}) = 0, \tag{3}$$

$$\boldsymbol{r}\in\Gamma_p : R_p = p(\boldsymbol{r}) - \overline{p}(\boldsymbol{r}) = 0, \tag{4}$$

$$\boldsymbol{r}\in\Gamma_Z : R_Z = \mathcal{L}_v(p(\boldsymbol{r})) - \frac{p(\boldsymbol{r})}{\overline{Z}_n(\boldsymbol{r})} = 0, \tag{5}$$

where the quantities $\overline{v}_n$, $\overline{p}$ and $\overline{Z}_n$ are, respectively, the imposed normal velocity, pressure and normal impedance. At the boundary at infinity Γ_∞ the Sommerfeld radiation condition [29] for outgoing waves is applied. This condition ensures that no acoustic energy is reflected at infinity and is expressed as

$$\lim_{|\boldsymbol{r}|\to\infty}\left(\sqrt{\boldsymbol{r}}\left(\frac{\partial p(\boldsymbol{r})}{\partial|\boldsymbol{r}|}+jkp(\boldsymbol{r})\right)\right)=0. \tag{6}$$

Solution of the Helmholtz equation (1) together with the associated boundary conditions (3)–(6) yields a unique acoustic pressure field $p(\boldsymbol{r})$. Once the pressure field is determined, derived acoustic quantities can be defined [28]:

- The acoustic particle velocity vector $\boldsymbol{v}(\boldsymbol{r})$ is proportional to the gradient of the pressure field, and can be written as

$$\boldsymbol{v}(\boldsymbol{r}) = \frac{j}{\rho\omega}\nabla p(\boldsymbol{r}). \tag{7}$$

- The active acoustic intensity vector $\boldsymbol{I}(\boldsymbol{r})$ representing the flow of acoustic energy is defined as

$$\boldsymbol{I}(\boldsymbol{r}) = \tfrac{1}{2}\Re(p(\boldsymbol{r})\boldsymbol{v}^*(\boldsymbol{r})) \tag{8}$$

with $\Re(x)$ the real part and x^* the complex conjugate of x.

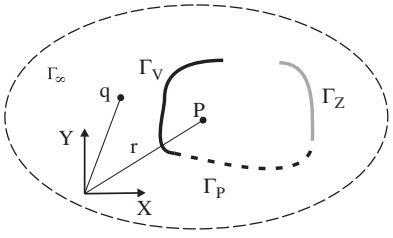

Fig. 1. A 2D unbounded acoustic problem.

3. The wave based method for acoustic radiation problems

The WBM [19] is a numerical modeling method based on an indirect Trefftz approach for the solution of steady-state acoustic problems in both bounded and unbounded problem domains. Instead of using simple approximating polynomials like in the FEM or BEM, the field variables are expressed as an expansion of wave functions which inherently satisfy the governing equation—in this case the Helmholtz equation (1). The degrees of freedom are the weighting factors of the wave functions in this expansion. It is an indirect approach, because these weighting factors are not the dynamic field variables themselves. Enforcing the boundary and continuity conditions using a weighted residual formulation yields a system of linear equations whose solution vector contains the wave function weighting factors.

The general modeling procedure consists of the following steps [30]:

(A) Partitioning into subdomains.
(B) Selection of the wave functions in the pressure expansion.
(C) Construction of the system of equations via a weighted residual formulation of the boundary conditions and the continuity conditions.
(D) Solution of the system of equations and postprocessing of the dynamic variables.

3.1. Partitioning into subdomains

When applied for bounded problems, a sufficient condition for the WB approximations to converge towards the exact solution is convexity of the considered problem domain [19]. In a general acoustic problem, the acoustic problem domain may be non-convex such that a partitioning into a number of convex subdomains is required.

If the WBM is applied to unbounded problems, an initial partitioning of the unbounded domain into a bounded and an unbounded region precedes the partitioning into convex subdomains [21]. Fig. 2 illustrates the principle. The unbounded acoustic problem domain is divided into two non-overlapping regions by a truncation curve Γ_t. The unbounded region exterior to Γ_t is considered as one acoustic subdomain.

In general, it is desirable to limit the domain partitioning to the minimum required to satisfy the rules above, because the introduction of additional interfaces increases the computational load. The aim is to divide the problem into a few, large subdomains. In cases with a complex problem geometry, the partitioning can be simplified by using a hybrid FE–WBM scheme, applying a FE model to discretize the geometrical details along the problem boundaries, while the bulk part of the problem domain is modeled using WBM subdomains, thus retaining to a large extent the efficiency of the WBM [31,32]. Moreover, a recently introduced multi-level WBM concept allows to simplify the partitioning and improve efficiency in several problems involving multiple scatterers [26] or inclusions [33].

3.2. Acoustic pressure expansion

The steady-state acoustic pressure field $p^{(\alpha)}(\boldsymbol{r})$ in an acoustic subdomain $\Omega^{(\alpha)}$ ($\alpha = 1 \dots N_\Omega$, with N_Ω the total number of subdomains, both bounded and unbounded) is approximated by a solution expansion $\hat{p}^{(\alpha)}(\boldsymbol{r})$:

$$p^{(\alpha)}(\boldsymbol{r}) \simeq \hat{p}^{(\alpha)}(\boldsymbol{r}) = \sum_{w=1}^{n_w^{(\alpha)}} p_w^{(\alpha)} \Phi_w^{(\alpha)}(\boldsymbol{r}) + \hat{p}_q^{(\alpha)}(\boldsymbol{r}) = \boldsymbol{\Phi}^{(\alpha)}(\boldsymbol{r}) \boldsymbol{p}_{\boldsymbol{w}}^{(\alpha)} + \hat{p}_q^{(\alpha)}(\boldsymbol{r}). \tag{9}$$

The wave function contributions $p_w^{(\alpha)}$ are the weighting factors for each of the selected wave functions $\Phi_w^{(\alpha)}$. Together they form the vector of degrees of freedom $\boldsymbol{p}_{\boldsymbol{w}}^{(\alpha)}$. The corresponding a priori defined wave functions are collected in the row vector $\boldsymbol{\Phi}^{(\alpha)}$. The set of all $n_W = \sum_{\alpha=1}^{N_\Omega} n_w^{(\alpha)}$ acoustic wave function contributions p_w is collected in the column vector $\boldsymbol{p}_{\boldsymbol{w}}$, while the row vector $\boldsymbol{\Phi}$ contains all n_W wave functions. $\hat{p}_q^{(\alpha)}$ represents a particular solution resulting from acoustic source terms $q^{(\alpha)}$ in the right hand side of the inhomogeneous Helmholtz equation (1).

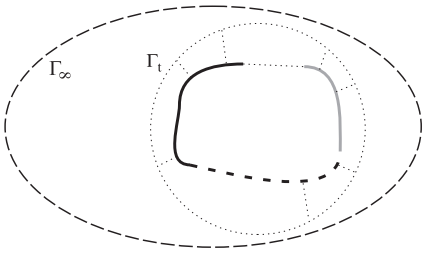

Fig. 2. A WB partitioning of the 2D unbounded problem. Subdomain interfaces are shown in dotted line (⋯).

3.2.1. Wave functions for a bounded subdomain

Each acoustic wave function $\Phi_w^{(\alpha)}(\boldsymbol{r})$ exactly satisfies the homogeneous part of the Helmholtz equation (1). For 2D bounded subdomains, the wave functions are constructed based on a solution of the Helmholtz equation (1) in Cartesian coordinates. Two types of wave functions are distinguished, the so-called *r*- and the *s*-set:

$$\sum_{w=1}^{n_w^{(\alpha)}} p_w^{(\alpha)} \Phi_w^{(\alpha)}(\boldsymbol{r}) = \sum_{w_r=1}^{n_{w_r}^{(\alpha)}} p_{w_r}^{(\alpha)} \Phi_{w_r}^{(\alpha)}(\boldsymbol{r}) + \sum_{w_s=1}^{n_{w_s}^{(\alpha)}} p_{w_s}^{(\alpha)} \Phi_{w_s}^{(\alpha)}(\boldsymbol{r}) \tag{10}$$

with $n_w^{(\alpha)} = n_{w_r}^{(\alpha)} + n_{w_s}^{(\alpha)}$. These wave functions are defined as

$$\Phi_w^{(\alpha)}(\boldsymbol{r}(x,y)) = \begin{cases} \Phi_{w_r}^{(\alpha)}(x,y) = \cos(k_{xw_r}^{(\alpha)} x) e^{-jk_{yw_r}^{(\alpha)} y}, \\ \Phi_{w_s}^{(\alpha)}(x,y) = e^{-jk_{xw_s}^{(\alpha)} x} \cos(k_{yw_s}^{(\alpha)} y), \end{cases} \tag{11}$$

The only requirement for the wave functions (11) to be exact solutions of (1) is

$$(k_{xw_r}^{(\alpha)})^2 + (k_{yw_r}^{(\alpha)})^2 = (k_{xw_s}^{(\alpha)})^2 + (k_{yw_s}^{(\alpha)})^2 = k^2. \tag{12}$$

As a result, an infinite number of wave functions (11) can be defined for expansion (9). Desmet [19] proposes to select the following wave number components:

$$(k_{xw_r}^{(\alpha)}, k_{yw_r}^{(\alpha)}) = \left(\frac{w_1^{(\alpha)} \pi}{L_x^{(\alpha)}}, \pm \sqrt{k^2 - (k_{xw_r}^{(\alpha)})^2} \right),$$

$$(k_{xw_s}^{(\alpha)}, k_{yw_s}^{(\alpha)}) = \left(\pm \sqrt{k^2 - (k_{yw_s}^{(\alpha)})^2}, \frac{w_2^{(\alpha)} \pi}{L_y^{(\alpha)}} \right) \tag{13}$$

with $w_1^{(\alpha)}$ and $w_2^{(\alpha)} = 0,1,2,\dots$. The dimensions $L_x^{(\alpha)}$ and $L_y^{(\alpha)}$ represent the dimensions of the (smallest) bounding rectangle, circumscribing the considered subdomain. With this selection for the wave numbers, the wave functions (11) represent a standing wave along one coordinate direction of the bounding box, multiplied with a propagating or evanescent component for the other direction.

An infinite number of wave functions (11) can be constructed using the wave numbers as detailed in (13). This series is truncated to $n_w^{(\alpha)}$ functions for subdomain $\Omega^{(\alpha)}$ by selecting the maximum values for $w_1^{(\alpha)}$ and $w_2^{(\alpha)}$:

$$\frac{w_{1,max}^{(\alpha)}}{L_x^{(\alpha)}} \approx \frac{w_{2,max}^{(\alpha)}}{L_y^{(\alpha)}} \geq \frac{Nk}{\pi} \tag{14}$$

with k the physical wave number in the problem under consideration. N is a truncation factor, relating the resolution in the WB description to the resolution of the physical problem. While the selection of the optimal value for N may depend on the specific problem, an important property of this rule is that it relates the number of functions in the expansion across the different subdomains such that a homogeneous approximation resolution is obtained throughout the problem. Lacking any specific information about the solution, this results in a balanced distribution of the computational effort over the different subdomains.

The particular solution $\hat{p}_q^{(\alpha)}$ for an acoustic source with source strength $q^{(\alpha)}$ inside a bounded subdomain is the free-field pressure field due to a cylindrical point source at source

position $(x_q^{(\alpha)}, y_q^{(\alpha)})$:

$$\hat{p}_q^{(\alpha)}(x,y) = \frac{\rho_0 \omega q^{(\alpha)}}{4} H_0^{(2)}(k r_q^{(\alpha)}) \tag{15}$$

with $r_q^{(\alpha)} = \sqrt{(x-x_q^{(\alpha)})^2 + (y-y_q^{(\alpha)})^2}$ and $H_0^{(2)}(\bullet)$ the zero-order Hankel function of the second kind. This particular solution is identical to the fundamental solution of the Helmholtz equation (1), with an amplitude factor of $-\rho_0 \omega q^{(\alpha)}/j$.

3.2.2. Wave functions for an unbounded subdomain

In addition to being homogeneous solutions of the Helmholtz equation, the wave functions for the unbounded domains are chosen to implicitly satisfy the Sommerfeld radiation condition (6). This removes the need to explicitly impose a radiation condition, similar as in the BEM. Herrera [34] shows that the following expansion $\hat{p_e}$, exterior to a circular truncation curve with radius R, yields a convergent set for the pressure field p_e, defined by a Neumann condition on the infinitely long cylinder with radius R:

$$p_e(r,\theta) \simeq \hat{p_e}(r,\theta) = p_{e,c0} H_0^{(2)}(kr) + \sum_{n=1}^{n_u} (p_{e,cn} H_n^{(2)}(kr)\cos(n\theta) + p_{e,sn} H_n^{(2)}(kr)\sin(n\theta)) \tag{16}$$

with r and θ the polar coordinates. $H_n^{(2)}(\bullet)$ is the n-th order Hankel function of the second kind. The contributions $p_{e,c0}$, $p_{e,cn}$ and $p_{e,sn}$ are determined by the velocity boundary condition. From this expansion, the following wave function set for unbounded domains is derived:

$$\Phi_w^{ub}(\boldsymbol{r}(r,\theta)) = \begin{cases} \Phi_{w_c}^{ub}(r,\theta) = H_w^{(2)}(kr)\cos(w\theta), \\ \Phi_{w_s}^{ub}(r,\theta) = H_w^{(2)}(kr)\sin(w\theta). \end{cases} \tag{17}$$

Due to the nature of the unbounded problem and the shape of the truncation, the unbounded wave functions are derived from a solution in polar coordinates. The resulting functions represent a harmonic distribution of the amplitude on the truncation, multiplied with the Hankel function $H_n^{(2)}(kr)$, describing the decay of an outgoing acoustic wave. Note that with this selection of the Hankel function, these functions always represent an outgoing wave, implicitly satisfying the Sommerfeld condition (6).

Using the functions (17) in the pressure expansion (9), the pressure in an unbounded subdomain can be represented. Analogous as for the bounded domains, the series of functions in the expansion has to be truncated. An equivalent rule imposing a desired resolution in the unbounded domain relative to the physical wave number yields

$$n_u = 2R_t N k \tag{18}$$

with n_u the highest order taken in the unbounded function set and R_t the radius of the truncation Γ_t. The physical interpretation of this rule is that a desired resolution of N halve wavelengths is imposed on the unbounded domain along the truncation Γ_t. Using this rule-of-thumb matches the spatial resolution of the approximation fields in all the WBM subdomains, both bounded and unbounded.

For modelling sources in unbounded acoustic domains, the particular solution for a cylindrical source (15) can be applied. Other source definitions for unbounded WB models, like the commonly used plane wave excitation, are discussed by Bergen [35].

3.2.3. Wave functions for a semi-unbounded subdomain

In many practical radiation problems, the unbounded domain is delimited by an infinitely extended rigid plane. Also for transmission cases the domain is split into two by a baffle (Fig. 3), yielding two semi-infinite subdomains. In order to introduce a rigid baffle line in a WB model, the baffle line has to be taken into account when partitioning the unbounded problem domain into a bounded region and an unbounded region, through the introduction of a truncation curve as shown in Fig. 3. The infinite baffle line extends into both the bounded and unbounded region. The part of the baffle inside the truncation curve is modelled by explicitly applying rigid normal velocity boundary conditions (3) with $\overline{v}_n = 0$, while the infinite part of the baffle, which is located in the unbounded region, is implicitly taken into account in the definition of the wave functions.

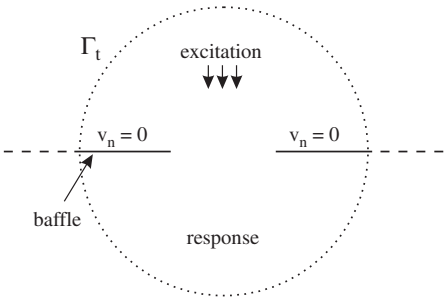

Fig. 3. Definition of a rigid baffle plane and corresponding WB truncation circle.

The baffled wave function set is based on the wave function sets resulting from the Neumann problems in circular coordinates (16). For wave functions to be suited for application in the semi-unbounded regions of a baffle model, the acoustic velocity normal to the baffle should be zero on the baffle, i.e. for $\theta = 0^\circ$ and 180°. The selected wave functions (16) are functions which are products of Hankel functions in the radial direction r with either a cosine or a sine function in the angular direction θ. The acoustic velocity, approximated by the derivatives of the applied wave functions, normal to the baffle, should be zero. This is the case for all functions which contain an angular cosine term, if the truncation circle is selected such that the center is situated on the baffle plane. Therefore, the functions with a sine term are omitted from the expansion, yielding the following basis function set for WB baffled calculations:

$$\Phi_w^{(ub)}(\boldsymbol{r}(r,\theta)) = \Phi_{w_c}^{(ub)}(r,\theta) = H_w^{(2)}(kr)\cos(w\theta). \tag{19}$$

In the case of transmission or diffraction problems, a separate set of basis functions of type (19) is defined for each of the two semi-infinite acoustic subdomains (one on each side of the baffle plane).

3.3. Acoustic wave model

The proposed expansion functions (11), (16) and (19) exactly satisfy the Helmholtz equation (1) inside the domain and the Sommerfeld radiation condition (6) at infinity. The boundary conditions and subdomain continuity are enforced through a weighted residual formulation. The residuals on the boundary conditions are given in (3)–(5), and the residuals enforcing continuity between two subdomains α and β can be written as

$$\boldsymbol{r} \in \Gamma_I : R_I^{(\alpha,\beta)} = \left(\frac{j}{\rho_0 \omega} \frac{\partial p^{(\alpha)}(\boldsymbol{r})}{\partial n^{(\alpha)}} - \frac{p^{(\alpha)}}{\overline{Z}_{int}}\right) + \left(\frac{j}{\rho_0 \omega} \frac{\partial p^{(\beta)}(\boldsymbol{r})}{\partial n^{(\beta)}} + \frac{p^{(\beta)}}{\overline{Z}_{int}}\right) \tag{20}$$

with $n^{(\alpha)}$ the local normal on the subdomain interface Γ_I, outwards of domain α and $\overline{Z}_{int}$ an impedance coupling factor, chosen as $\rho_0 c$ [30]. Note that this continuity condition is enforced on each domain, for each interface, yielding two continuity conditions over each subdomain interface.

For each subdomain, the error functions are orthogonalized with respect to a weighting function $\tilde{p}^{(\alpha)}$ or its derivative. The weighted residual formulation, applying the introduced error functions, is expressed as

$$\int_{\Gamma_v^{(\alpha)}} \tilde{p}^{(\alpha)}(\boldsymbol{r}) R_v^{(\alpha)}(\boldsymbol{r})\, \mathrm{d}\Gamma + \int_{\Gamma_Z^{(\alpha)}} \tilde{p}^{(\alpha)}(\boldsymbol{r}) R_Z^{(\alpha)}(\boldsymbol{r})\, \mathrm{d}\Gamma + \int_{\Gamma_p^{(\alpha)}} -\mathcal{L}_v^{\alpha}(\tilde{p}^{(\alpha)}(\boldsymbol{r})) R_p^{(\alpha)}(\boldsymbol{r})\, \mathrm{d}\Gamma + \sum_{\beta=1,\beta\neq\alpha}^{N_\Omega} \int_{\Gamma_I^{(\alpha,\beta)}} \tilde{p}^{(\alpha)}(\boldsymbol{r})\, R_I^{(\alpha,\beta)}(\boldsymbol{r})\, \mathrm{d}\Gamma = 0. \tag{21}$$

Like in the Galerkin weighting procedure, used in the FEM, the weighting functions $\tilde{p}^{(\alpha)}$ are expanded in terms of the same set of acoustic wave functions used in the pressure expansions (9) and (16)

$$\tilde{p}^{(\alpha)}(\boldsymbol{r}) = \sum_{a=1}^{n_a^{(\alpha)}} \tilde{p_a}^{(\alpha)} \Phi_a^{(\alpha)}(\boldsymbol{r}) = \boldsymbol{\Phi}^{(\alpha)}(\boldsymbol{r}) \tilde{\boldsymbol{p}}_{\boldsymbol{w}}^{(\alpha)}. \tag{22}$$

From here onwards, the position dependence of the vectors is omitted in the notations.

Substitution of the pressure expansions (9) and (16) and the weighting function expansion (22) into the weighted residual formulation (21) yields

$$\begin{aligned}\tilde{\boldsymbol{p}}_{\boldsymbol{w}}^{(\alpha)T}[&\boldsymbol{C}_{\boldsymbol{aa}}^{(\alpha,1)} \boldsymbol{p}_{\boldsymbol{w}}^{(1)} + \cdots + \boldsymbol{C}_{\boldsymbol{aa}}^{(\alpha,\alpha-1)} \boldsymbol{p}_{\boldsymbol{w}}^{(\alpha-1)} + \boldsymbol{A}_{\boldsymbol{aa}}^{(\alpha)}\, \boldsymbol{p}_{\boldsymbol{w}}^{(\alpha)} \\ &+ \boldsymbol{C}_{\boldsymbol{aa}}^{(\alpha,\alpha+1)}\, \boldsymbol{p}_{\boldsymbol{w}}^{(\alpha+1)} + \cdots + \boldsymbol{C}_{\boldsymbol{aa}}^{(\alpha,N_\Omega)}\, \boldsymbol{p}_{\boldsymbol{w}}^{(N_\Omega)} \\ &- \boldsymbol{f}_{\boldsymbol{a}}^{(\alpha,1)} - \cdots - \boldsymbol{f}_{\boldsymbol{a}}^{(\alpha,\alpha-1)} - \boldsymbol{f}_{\boldsymbol{a}}^{(\alpha)} - \boldsymbol{f}_{\boldsymbol{a}}^{(\alpha,\alpha+1)} - \cdots - \boldsymbol{f}_{\boldsymbol{a}}^{(\alpha,N_\Omega)}] = 0.\end{aligned} \tag{23}$$

For a detailed description of the system matrices, the reader is referred to Desmet [19]. Due to the oscillatory behavior of the wave functions, care should be taken when evaluating the integrals in (21). Standard Gaussian quadrature has proven to be adequate [36], providing sufficient integration points are used. For all calculations, a minimum of eight integration points per wavelength (of the wave functions) is used.

Since the weighted residual formulation (21) should hold for any weighting function $\tilde{p}^{(\alpha)}$, the expressions between the square brackets in Eq. (23) must be zero. This yields a set of $n_w^{(\alpha)}$ linear equations in the n_W unknown wave function contribution factors. One such matrix equation is obtained for each subdomain. Combination of the N_Ω systems yields the acoustic WB model, consisting of n_W algebraic equations in the n_W unknown wave function contribution factors:

$$[\boldsymbol{A}_{\boldsymbol{aa}}]\{\boldsymbol{p}_{\boldsymbol{w}}\} = \{\boldsymbol{b}\}. \tag{24}$$

3.4. Solution and postprocessing

The resulting model (24) can be solved for the unknown wave function contributions p_w. The final step in the modeling process is backsubstitution of these contribution factors into the pressure expansions (9), yielding an analytical description of the approximated dynamic pressure field $\hat{p}$.

3.5. WBM model properties

Where the FEM and BEM use simple polynomials in a fine discretization to describe the dynamic variables, the WBM uses wave functions in a coarse partitioning of the domain. As a consequence, the WBM does not suffer from pollution errors and relatively few degrees of freedom are needed to accurately represent the dynamic field. The downside of this is the requirement of convex subdomains (for the bounded domains), deteriorating the efficiency when the problem geometry is complex and extensive partitioning is needed.

As an added advantage, derived quantities like acoustic velocity and intensity can be easily calculated from the analytic derivatives of the basis functions. Because of the wave-like nature of those basis functions, there is no loss of accuracy for derived variables, since the derivatives have a similar spatial resolution.

The use of a Trefftz basis typically leads to ill-conditioned systems [37]. Therefore, the highly oscillatory integrals (21) should be evaluated with care to ensure the matrix coefficients are determined to high accuracy. The use of a Gauss–Legendre quadrature with a fixed number of integration points per wavelength (of the approximation functions) allows an efficient integration meeting the desired accuracy. Furthermore, [19] proves that the system resulting from a WB model meets the so-called Picard conditions [38], indicating that an accurate solution can be obtained despite the unfavorable condition number. The results of similar Picard tests performed for unbounded and semi-unbounded problems support the observations made by [19] and hence indicate that the introduction of the proposed set of unbounded and semi-unbounded basis functions in the WBM approach does not adversely affect the practical convergence of the method.

As for the BE method and in contrast with the FE method, the WBM yields a fully populated matrix, whose elements are complex and which cannot be decomposed into frequency independent submatrices. However, because the system is substantially smaller, computation times are generally lower as compared to the element based methods. These advantageous computation times, combined with the good accuracy of the WBM, result in an excellent convergence rate and a computational efficiency which is superior to the FEM and BEM for a range of steady-state dynamic problems [20,22–27], allowing the method to tackle problems at higher frequencies.

4. Numerical examples

This section discusses two numerical examples. In a first example, the proposed formulation is verified by comparison with an analytical solution. The problem considered is a vibrating piston in a baffle plane. A second example looks at the transmission through an aperture in a baffle, shielded by a plate.

4.1. A vibrating piston in a baffle plane

4.1.1. Problem definition

The WBM approach for modeling baffled problems is applied to analyze a vibrating piston in a baffle plane (Fig. 4). This allows for validation of the method by comparing the obtained pressure field with an analytical solution of this problem, obtained by evaluation of the Rayleigh integral formulation. The piston width is 1 m, the acoustic fluid is air (c=340 m/s, $\rho_0 = 1.225$ kg/m^3). The piston is vibrating with a unit velocity ($\overline{v} = 1$ m/s).

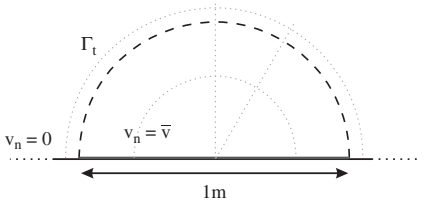

Fig. 4. Vibrating piston with WB domain partitioning indicated in dashed line (- -). Results are processed on the dotted lines (···).

4.1.2. Model descriptions

Wave based model: The truncation circle is chosen to exactly span the piston, yielding a truncation radius of 0.5 m, as shown in Fig. 4. The bounded subdomain is modelled using one WB subdomain.

Analytical solution: The analytical solution of the vibrating piston problem can be obtained by solving the Rayleigh integral [28]. For this 2D baffled problem with velocity excitation this yields

$$p(\boldsymbol{r}) = j\rho_0\omega \int_{\Gamma_a} v_n(\boldsymbol{r}) G_{1/2}(\boldsymbol{r},\boldsymbol{r_a})\, \mathrm{d}\Gamma \tag{25}$$

with $G_{1/2}(\boldsymbol{r},\boldsymbol{r_a})$ the 2D halfspace Green's kernel function

$$G_{1/2}(\boldsymbol{r},\boldsymbol{r_a}) = 2G(\boldsymbol{r},\boldsymbol{r_a}) = -\frac{j}{2} H_0^{(2)}(k|\boldsymbol{r}-\boldsymbol{r_a}|), \tag{26}$$

where $G(\boldsymbol{r},\boldsymbol{r_a})$ is the regular 2D Green's function. The integration domain Γ_a is the vibrating surface of the piston. A Gauss–Legendre integration scheme is used for the evaluation of the integral. The number of integration points was increased until the analytical solution converged to the machine precision, in this case requiring around 1000 integration points.

4.1.3. Results

Fig. 5 shows the contours of the real part of the resulting pressure field at 1000 Hz ($ka \approx 18$ with a being a characteristic dimension of the problem, in casu the piston width). This result is obtained using a WB model consisting of 100 wave functions. For comparison with the analytical solution, the pressure is plotted along a line starting from the center of the piston, at an angle of 60° and 90° with the baffle. This is shown in Fig. 6(a) and (b), respectively, along with the relative pressure difference ΔP_{rel}:

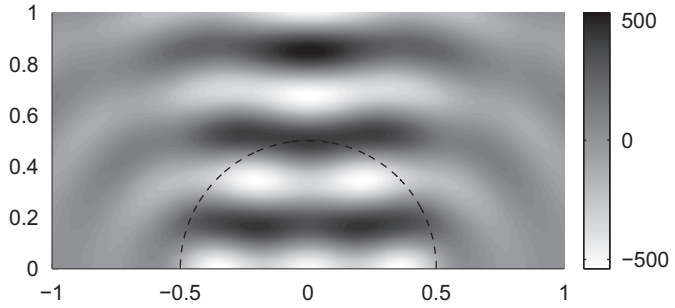

Fig. 5. Contour field at 1000 Hz, real part of the pressure [Pa].

$$\Delta P_{rel} = \frac{\|\hat{p} - p_{ref}\|}{\|p_{ref}\|}, \tag{27}$$

where p_{ref} is the analytically calculated reference pressure; $\|x\|$ denotes the amplitude of the complex number x. It can be observed that the WB result matches the analytical solution, obtained from the Rayleigh integral.

Fig. 7(a) and (b) shows the real part of the pressure and the relative pressure difference along a circle with radius 0.3 m and 0.55 m respectively, the first curve being situated inside the bounded subdomain, the second in the unbounded. Again, a good agreement with the analytical solution can be observed. This is further illustrated in Fig. 8, where the error evolution is shown for an increasing number of degrees of freedom in the model. The error shown is the mean relative error on the pressure amplitude, evaluated along both a line through the origin and an arc at radius 0.65 m. It can be clearly observed that the WB model converges to the analytical solution, and excellent accuracy is obtained already with few (< 100) functions.

4.2. Diffraction through a shielded baffle aperture

4.2.1. Problem definition

In a second numerical example the formulations are applied to a diffraction problem, consisting of an aperture in a baffle, shielded by a plate. The aperture is 0.5 m wide. The shielding surface, positioned 0.2 m under the baffle, is 0.6 m wide. The acoustic fluid is the same as in the previous example. The problem is excited by a point source q with amplitude 1 Pa above and right of the aperture. Fig. 9 shows the problem and the WB domain decomposition.

4.2.2. Model description

The part above the baffle is modeled using three bounded and one semi-unbounded WB subdomain, for the lower part eight bounded and one semi-unbounded subdomain are used. The smallest constructed wave model uses 134 bounded wave functions and two times 64 semi-unbounded wave functions. This model is refined until it consists of 2216 bounded and 578 semi-unbounded functions.

4.2.3. Results

Figs. 10 and 11 show, respectively, the real part of the pressure and the active intensity field resulting from the point source

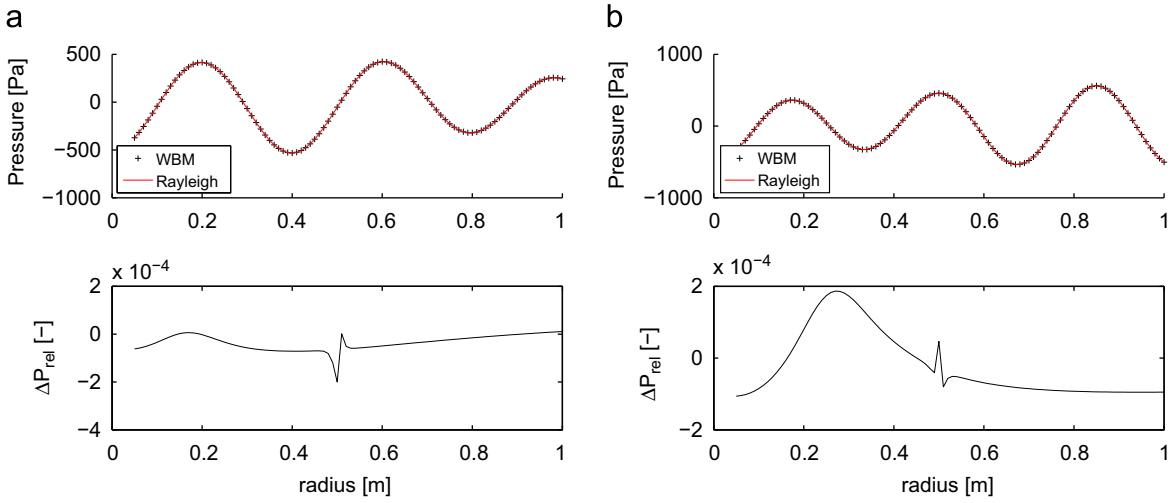

Fig. 6. Real part of the pressure and relative error at 1000 Hz ($ka \approx 18$). (a) Line at $\theta = \pi/3$. (b) Line at $\theta = \pi/2$.

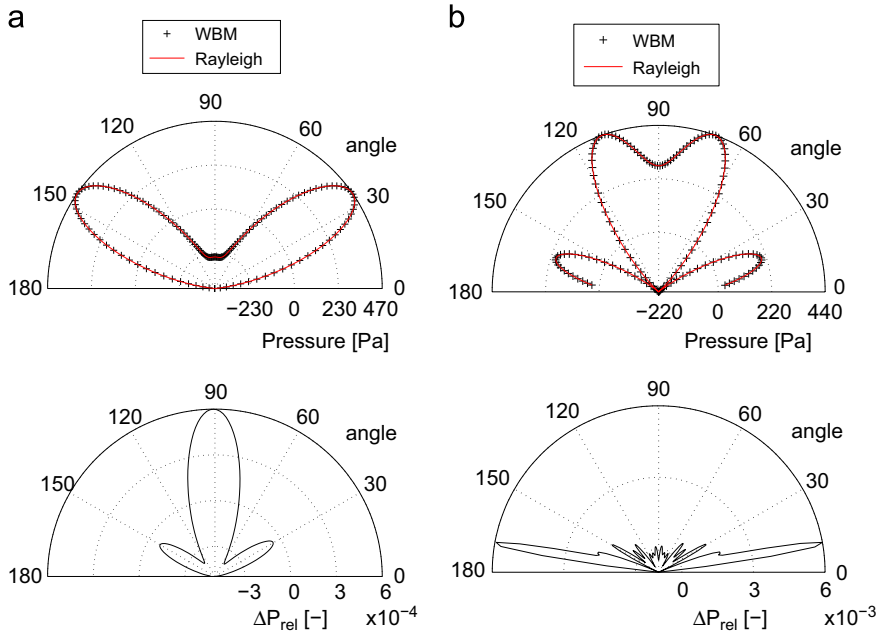

Fig. 7. Real part of the pressure and relative error at 1000 Hz ($ka \approx 18$). (a) Circle at $r=0.3$ m. (b) Circle at $r=0.55$ m.

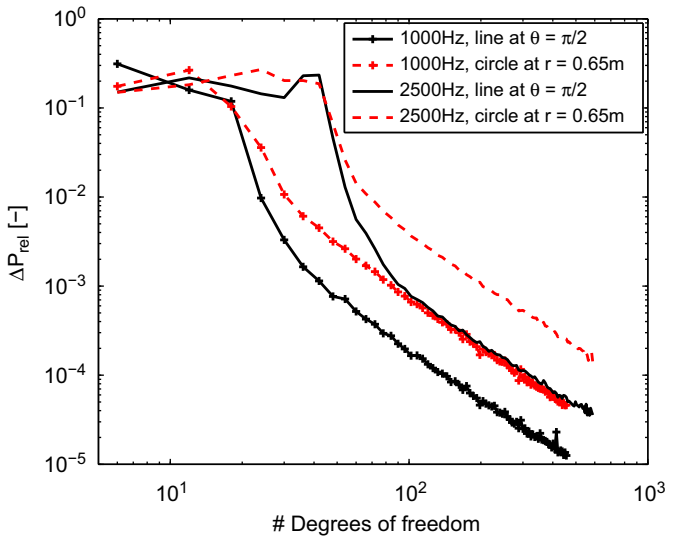

Fig. 8. Relative pressure error convergence at 1000 Hz ($ka \approx 18$) and 2500 Hz ($ka \approx 46$) for the line at $\theta = \pi/2$ and the circle at $r=0.65$ m.

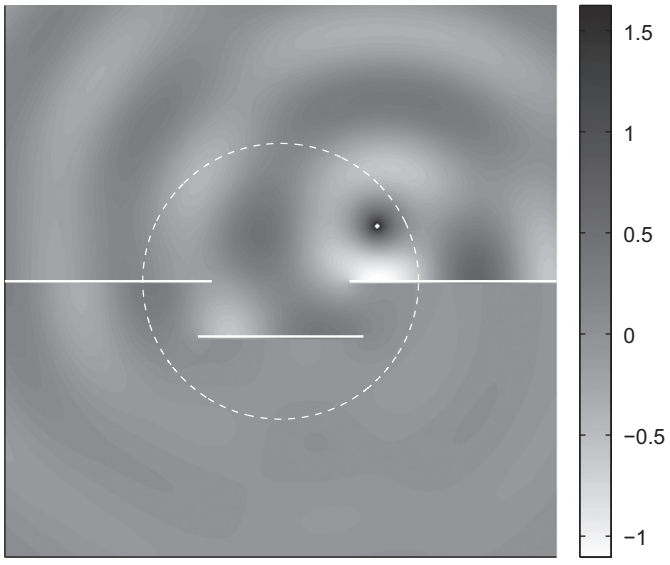

Fig. 10. Contour field at 700 Hz, real part of the pressure (Pa).

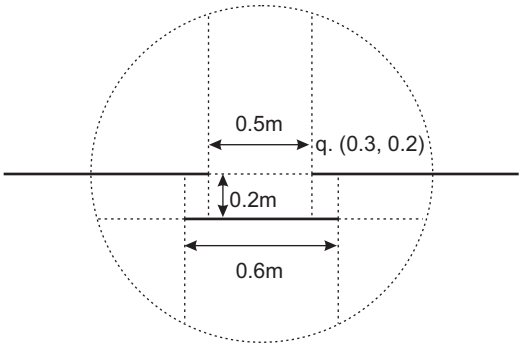

Fig. 9. Problem definition of the shielded aperture in a baffle, indicating the WB domain partitioning in dotted line (···).

excitation at a frequency of 700 Hz ($ka \approx 8$ with $a=0.6$ m). It is clear that the obtained pressure field satisfies the imposed boundary conditions: pressure contours are perpendicular to the rigid walls, and the inter-domain continuity is respected. The rigid baffle in the unbounded part, which is introduced by the choice of the semi-unbounded wave functions, is also correctly represented: pressure contours are perpendicular to it and no intensity is flowing through. The evolution of the relative error on both pressure (ΔP_{rel}) and active intensity ($\Delta I_{act,rel}$), for increasing number of wave functions in the model, is shown in Fig. 12. The errors are calculated using Eq. (27) for the pressure and equivalent for the intensity, and subsequently averaged over a square around the problem geometry (same area as the contour field shown in Figs. 10 and 11). A large WB model is taken as a reference for the error calculation. A good convergence is observed, both for the pressure and for the active intensity, where the rate is similar for both, since derived quantities like velocity

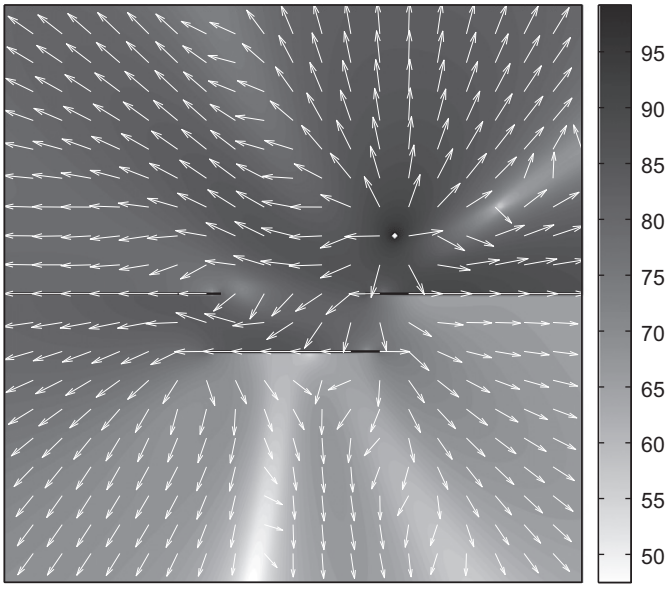

Fig. 11. Vector field at 700 Hz ($ka \approx 8$), active intensity (dB re 1 pW).

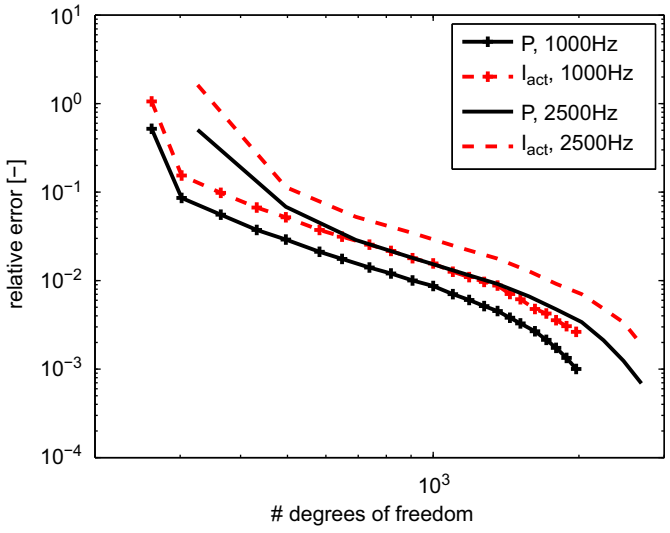

Fig. 12. Relative pressure and active intensity error convergence at 1000 Hz ($ka \approx 11$) and 2500 Hz ($ka \approx 28$).

and active intensity can be computed by analytic derivation of the basis functions.

5. Conclusions

This paper discusses an extension of wave based method (WBM) for the treatment of acoustic problems in semi-infinite domains. To efficiently model these domains, a function set is proposed that not only satisfies the Helmholtz equation, but also the Sommerfeld radiation condition and the velocity condition on the rigid baffle plane. The absence of pollution errors and the small system result in a good prediction accuracy and a high convergence rate.

The resulting technique is validated through the study of a pulsating piston in a baffle, allowing for comparison with an analytical formulation of the solution. It is shown that the WBM matches this reference solution with great accuracy. A second numerical example illustrates the potential of the WBM for more complex diffraction problems. The problem studied consists of an aperture in a baffle, shielded by a rigid surface. The examples considered illustrate the good convergence rate of the WBM, both when considering pressure and derived quantities such as acoustic intensity. Due to the wave-like nature of the basis functions, there is no decrease in accuracy when studying derived quantities. This good convergence and associated computational efficiency enables to use the technique for practical mid-frequency problems.

Acknowledgments

The research of Bart Bergen is funded by a Ph.D. grant of the Institute for the Promotion of Innovation through Science and Technology in Flanders (IWT-Vlaanderen) and Bert Van Genechten is a Doctoral Fellow of the Fund for Scientific Research — Flanders (F.W.O.), Belgium. The authors also gratefully acknowledge the ITN Marie Curie project GA-214909 "MID-FREQUENCY — CAE Methodologies for Mid-Frequency Analysis in Vibration and Acoustics" and the FWO project G.0316.09 — "Numerical methods for the accurate aurelisation and evaluation of binaural human perception of broadband acoustic and vibro-acoustic phenomena".

References

[1] Zienkiewicz OC, Taylor RL, Zhu JZ. The finite element method—Vol. 1: its basis & fundamentals. 6th ed. Butterworth-Heinemann; 2005.
[2] Harari I. A survey of finite element methods for time-harmonic acoustics. Computer Methods in Applied Mechanics and Engineering 2006;195:1594–607.
[3] Thompson LL. A review of finite element methods for time-harmonic acoustics. Journal of the Acoustical Society of America 2006;119:1315–30.
[4] Givoli D, Vigdergauz S. Artificial boundary conditions for 2d problems in geophysics. Computer Methods in Applied Mechanics and Engineering 1993;110(1–2):87–101.
[5] Coyette JP, Van den Niewenhof B. A conjugated infinite element method for half-space acoustic problems. Journal of the Acoustical Society of America 2000;108:1464–73.
[6] Zschiedrich L, Klose R, Schädle A, Schmidt F. A new finite element realization of the perfectly matched layer method for Helmholtz scattering problems on polygonal domains in two dimensions. Journal of Computational and Applied Mathematics 2006;188(1):12–32.
[7] Von Estorff O. Boundary elements in acoustics: advances and applications. WIT Press; 2000.
[8] Bouillard P, Ihlenburg F. Error estimation and adaptivity for the finite element method in acoustics: 2D and 3D applications. Computer Methods in Applied Mechanics and Engineering 1999;176:147–63.
[9] Marburg S. Six boundary elements per wavelength: Is that enough? Journal of Computational Acoustics 2002;10:25–51.
[10] Boyd J. Chebyshev and Fourier spectrum methods. 2nd ed. New York: Dover; 2001.
[11] Bialecki B, Karageorghis A. Spectral Chebyshev–Fourier collocation for the Helmholtz and variable coefficient equations in a disk. Journal of Computational Physics 2008;227(19):8588–603.
[12] Trefftz E. Ein Gegenstück zum Ritzschen Verfahren. In: Proceedings of the 2nd international congress on applied mechanics, Zurich, Switzerland, 1926. p. 131–7.
[13] Koopmann G, Song L, Fahnline J. A method for computing acoustic fields based on the principle of wave superposition. Journal of the Acoustical Society of America 1989;86:2433–8.
[14] Chen JT, Lee YT, Yu SR, Shieh SC. Equivalence between the Trefftz method and the method of fundamental solution for the annular Green's function using the addition theorem and image concept. Engineering Analysis with Boundary Elements 2009;33(5):678–88.
[15] Alves CJ, Valtchev SS. Numerical comparison of two meshfree methods for acoustic wave scattering. Engineering Analysis with Boundary Elements 2005;29(4):371–82.
[16] Li ZC, Young LJ, Huang HT, Liu YP, Cheng AHD. Comparisons of fundamental solutions and particular solutions for Trefftz methods. Engineering Analysis with Boundary Elements 2010;34(3):248–58.
[17] Reutskiy S. A Trefftz type method for time-dependent problems. Engineering Analysis with Boundary Elements 2004;28(1):13–21.
[18] Kita E, Ikeda Y, Kamiya N. Indirect Trefftz method for boundary value problem of Poisson equation. Engineering Analysis with Boundary Elements 2003;27(8):825–33.

[19] Desmet W. A wave based prediction technique for coupled vibro-acoustic analysis. PhD thesis 98D12, KULeuven, division PMA; 1998 URL 〈http://www.mech.kuleuven.be/mod/wbm/phd_dissertations〉.
[20] Vanmaele C, Vandepitte D, Desmet W. An efficient wave based prediction technique for dynamic plate bending problems with corner stress singularities. Computer Methods in Applied Mechanics and Engineering 2009;198(30–32):2227–45.
[21] Pluymers B, Van Hal B, Vandepitte D, Desmet W. Trefftz-based methods for time-harmonic acoustics. Archives of Computational Methods in Engineering 2007;14(4):343–81.
[22] Desmet W, Van Hal B, Sas P, Vandepitte D. A computationally efficient prediction technique for the steady-state dynamic analysis of coupled vibro-acoustic systems. Advances in Engineering Software 2002;33:527–40.
[23] Sas P, Desmet W, Vandepitte D. A wave-based prediction technique for vibroacoustics: comparison with the finite-element technique and experimental validation. Journal of the Acoustical Society of America 1998;103:2770.
[24] Pluymers B, Desmet W, Vandepitte D, Sas P. Application of an efficient wave based prediction technique for the analysis of vibro-acoustic radiation problems. Journal of Computational and Applied Mathematics 2004;168:353–64.
[25] Pluymers B, Desmet W, Vandepitte D, Sas P. On the use of a wave based prediction technique for steady-state structural-acoustic radiation analysis. Journal of Computer Modeling in Engineering & Sciences 2005;7(2):173–84.
[26] Van Genechten B, Bergen B, Vandepitte D, Desmet W. A Trefftz-based numerical modelling framework for Helmholtz problems with complex multiple scatterer configurations. Journal of Computational Physics 2010;229(18):6623–43.
[27] Bergen B, Van Genechten B, Vandepitte D, Desmet W. An efficient Trefftz-based method for three-dimensional Helmholtz problems in unbounded domains. Computer Modeling in Engineering & Sciences 2010;61(2):155–75.
[28] Pierce A. Acoustics: an introduction to its physical principles and applications. McGraw-Hill series in mechanical engineering. McGraw-Hill; 1981.
[29] Colton D, Kress R. Inverse acoustic and electromagnetic scattering theory. 2nd ed. Berlin, Heidelberg, New York: Springer-Verlag; 1998.
[30] Pluymers B. Wave based modelling methods for steady-state vibro-acoustics. PhD thesis 2006D04, KULeuven, division PMA; 2006. URL 〈http://www.mech.kuleuven.be/mod/wbm/phd_dissertations〉.
[31] van Hal B, Desmet W, Vandepitte D. Hybrid finite element—wave-based method for steady-state interior structural-acoustic problems. Computers & Structures 2005;83(2–3):167–80.
[32] Van Genechten B, Pluymers B, Vandepitte D, Desmet W. A hybrid wave based—modally reduced finite element method for the efficient analysis of low- and mid-frequency car cavity acoustics. SAE International Journal of Passenger Cars—Mechanical Systems 2009;2(1):1494–504.
[33] Genechten BV, Vergote K, Vandepitte D, Desmet W. A multi-level wave based numerical modelling framework for the steady-state dynamic analysis of bounded Helmholtz problems with multiple inclusions. Computer Methods in Applied Mechanics and Engineering 2010;199(29–32):1881–905.
[34] Herrera I. Boundary methods: an algebraic theory. London: Pitman Adv. Publ. Program; 1984.
[35] Bergen B, Van Genechten B, Pluymers B, Vandepitte D, Desmet W. Efficient wave based models for acoustic scattering and transmission problems using point source and plane wave excitation. In: Proceedings of the fourteenth international congress on sound and vibration (ICSV14), Cairns, Australia, 2007.
[36] Deckers E, Drofmans B, Van Genechten B, Bergen B, Vandepitte D, Desmet W. Spline-based boundaries: a first step towards generic geometric domain descriptions for efficient mid-frequency acoustic analysis using the wave based method. Journal of Computational and Applied Mathematics 2011;235(8):2679–93.
[37] Li ZC, Huang HT. Study on effective condition number for collocation methods. Engineering Analysis with Boundary Elements 2008;32(10):839–48.
[38] Varah J. A practical examination of some numerical methods for linear discrete ill-posed problems. SIAM Review 1979;21:100–11.